Hemoglobin Allostery: New Views on Old Players

ARTICLE *in* JOURNAL OF MOLECULAR BIOLOGY · DECEMBER 2012

Impact Factor: 4.33 · DOI: 10.1016/j.jmb.2012.12.018 · Source: PubMed

3 AUTHORS, INCLUDING:

Adriana Erica Miele

Sapienza University of Rome

55 PUBLICATIONS **1,130** CITATIONS

SEE PROFILE

jmb Article

Hemoglobin Allostery: New Views on Old Players

Adriana Erica Miele, Andrea Bellelli and Maurizio Brunori

Department of Biochemical Sciences and Istituto Pasteur-Fondazione Cenci Bolognetti, *"Sapienza" University of Rome, P.le Aldo Moro 5, 00185 Rome, Italy*

Correspondence to Maurizio Brunori: *Department of Biochemical Sciences, "Sapienza" University of Rome, P.le Aldo Moro 5, 00185 Rome, Italy. maurizio.brunori@uniroma1.it*
http://dx.doi.org/10.1016/j.jmb.2012.12.018
Edited by S. Edelstein

Abstract

Proteins are dynamic molecular machines whose structure and function are modulated by environmental perturbations and natural selection. Allosteric regulation, discovered in 1963 as a novel molecular mechanism of enzymatic adaptation [Monod, Changeux & Jacob (1963). *J. Mol. Biol.* **6**, 306–329], seems to be the leit motiv of enzymes and metabolic pathways, enabling fine and quick responses toward external perturbations. Hemoglobin (Hb), the oxygen transporter of all vertebrates, has been for decades the paradigmatic system to test the validity of the conformational selection mechanism, the conceptual innovation introduced by Monod, Wyman and Changeux. We present hereby the results of a comparative analysis of structure, function and thermodynamics of two extensively investigated hemoglobins: human HbA and trout HbI. They represent a unique and challenging comparison to test the general validity of the stereochemical model proposed by Perutz. Indeed both proteins are ideal for the purpose being very similar yet very different. In fact, T-HbI is a low-ligand-affinity cooperative tetrameric Hb, insensitive to all allosteric effectors. This remarkable feature, besides being physiologically sound, supports the stereochemical model, given that the six residues identified in HbA as responsible for the Bohr and the 2,3-di-phosphoglycerate effects are all mutated. Comparison of the three-dimensional structures of HbA and T-HbI allows unveiling the molecular mechanism whereby the latter has a lower O_2 affinity. Moreover, the energetic balance sheet shows that the salt bridges breaking upon allosteric quaternary transition are important yet insufficient to account for the free energy of heme–heme interactions in both hemoglobins.

Introduction

When the Monod–Wyman–Changeux (MWC) model was first formulated,[1] structural biology was in its infancy, and apart for hemoglobin (Hb), there were essentially no other complex proteins whose structure had been solved in order to test this new idea. Nowadays, every Biochemistry textbook reports that allostery arises when a change in shape of an active site is coupled to a quaternary structural transition of an oligomeric protein, as initially discovered by comparing the three-dimensional structure of deoxy and oxy/CO Hb.[2,3] The preexisting equilibrium between states is prone to a shift because the free-energy landscape of proteins is dynamic and binding events can bias the relative populations by selecting preferentially one conformer.[4,5] The most popular attempt to correlate structural features at quasi-atomic level with function and mechanism in HbA was Max F. Perutz stereochemical model.[2] In a seminal work, he presented a comprehensive picture to explain a wealth of functional data based on the structures of liganded and unliganded HbA, solved in Cambridge.[6,7] Despite the relatively low resolution, Perutz singled out some key features and attempted to account quantitatively for Hb's cooperativity and allostery, testing consistency between structure and the basic idea of the MWC theory.

In this paper, we present an original analysis of the allosteric properties of two "classical" extensively investigated hemoglobins, namely, the major isoform of human hemoglobin (HbA)[8] and one of the main isoforms of trout's blood (called T-HbI).[9] Indeed the two proteins share a bunch of common features such as the globin fold, the quaternary assembly, reversible O_2 binding and cooperativity. Nevertheless, they differ in ligand affinity, binding of allosteric effectors, stability of the quaternary

Table 1. The buried surface areas (Å^2) for deoxy and CO derivatives of HbA and T-HbI

	Buried surface area (Å^2)			
	HbA deoxy (2dn2)	T-HbI deoxy (1out)	HbA CO (2dn3)	T-HbI CO (1ouu)
Interfaces $\alpha_1\beta_1$ and $\alpha_2\beta_2$	3309.0	3445.6	3634.8	3538.4
Interfaces $\alpha_1\beta_2$ and $\alpha_2\beta_1$	2708.6	2576.4	2124.6	3189.6

assembly and more.[9,10] A quantitative comparison of structure and function of these two evolutionarily distant hemoglobins is possible because Tame *et al*. solved the three-dimensional structure of deoxy and CO-bound trout HbI (T-HbI, herein)[11] and also published high-resolution structures of HbA (deoxygenated, oxygenated and CO bound).[12]

HbA and T-HbI are ideal for the purpose being "very similar yet very different". Apart from cooperative O_2 binding even under isoionic conditions,[13] T-HbI is quite peculiar since O_2 affinity and cooperativity are totally independent of classical heterotropic effectors given that there is no Bohr effect, no effect of organic phosphates [2,3-di-phosphoglycerate (DPG), adenosine triphosphate (ATP), inositol hexaphosphate (IHP) and pyridoxal 5′-phosphate (PLP)] and only a negligible effect of chloride, orthophosphate and Na^+ that increases $p_{1/2}$ from 12–13 mmHg to 14–15 mmHg at 0.2–0.3 M.[13–15] There is no kinetic, equilibrium and spectroscopic evidence for αβ subunit heterogeneity, and the tetramer is approximately 100-fold more stable than liganded HbA.[16,17] In a nutshell, T-HbI has none of the classical heterotropic control properties typical of most other tetrameric hemoglobins, such as the Bohr effect and the DPG control, yet is cooperative in O_2 and CO binding.

The differences in amino acid sequence between T-HbI and HbA[18] are clearly crucial as principal structural determinants of function. Therefore, we took the opportunity to test quantitatively the energetics of the stereochemical model of Perutz[2,19] and specifically the role of a finite number of residues and their molecular interactions in accounting for homotropic and heterotropic effects in HbA. Based on a careful analysis of the crystallographic coordinates of HbA (at 1.25 Å) and of T-HbI (at 2.3–2.5 Å) obtained by Tame *et al*. and Park *et al*. on the deoxy and ligand-bound states,[11,12] we highlight that the specific role of a limited number of residues in controlling the allosteric properties of Hb is essentially correct and provides evidence that ligand-linked salt bridges are necessary but not sufficient to account for the energetics of the quaternary constraint. We give hereby explicit credit to a few among the many groups that contributed fundamental knowledge over the years[20–26] and apologize with all the others that we could not quote, for reasons of space.

Results and Discussion

A glance at the structures of human and trout hemoglobins

The structures of the deoxy and CO-bound derivatives of HbA[12] are superimposable to those

Fig. 1. The structures of T-HbI (2.3 and 2.5 Å resolution) are represented in ribbon style, and those of HbA (1.25 Å resolution) are represented in gray-worm style. All amino acids within 6.0 Å from the hemes are represented in stick, and those highlighted are named with one-letter code. The structures of the two hemoglobins have been optimally superimposed with SSM,[43] based on the BGH frame. (a) The heme pockets in the deoxygenated state. α subunits: representation of the superposition of the α subunits (in salmon), with magnified views of the distal side (top box) and proximal side (bottom box). In the proximal side, T-HbI shows a more constrained F helix, with a larger pass than in HbA. On the distal side of T-HbI, the major feature is the presence of αTrp46(CE4) at the heme entrance, making a H-bond with one propionate; this residue may gate or slow down the access of a ligand. Although the heme iron-proximal His distance in T-HbI and in HbA is the same, the heme appears less bent in the former protein. β subunits: representation of the superposition of the β subunits (light green), with magnified views of the distal side (top box) and proximal side (bottom box). In T-HbI, the heme is markedly domed with the iron pulled by the proximal His92(F8) helped by Thr91(F7), which lies parallel with it and makes a H-bond with one propionate. This double constraint may have an effect on the access of an incoming ligand. In addition, the distal side is more hydrophobic, as can be noticed by the substitutions highlighted [Val66(E10) and Ile67(E11)]. (b) The heme pockets in the CO state, same orientation as in (a). α-CO subunits: representation of the superposition of the α subunits (orange), with magnified views of the distal side (top box) and proximal side (bottom box). On the latter, there are virtually no differences between HbA and T-HbI; on the other hand, on the distal side, the clamping action on the propionate by αTrp46(CE4) is reinforced by the adjacent αHis45(CE3). It is worth of notice that distal His59(E7) does not contact the oxygen atom of Fe-bound CO and points toward the exterior in the place left free by the absence of Lys61(E10), which in T-HbI is substituted by Ile62(E10). β-CO subunits: representation of the superposition of the β subunits (lime), with magnified views of the distal side (top box) and proximal side (bottom box). In this case, a proximal effect is more prominent, the F helix being pivoted toward the bottom by 0.9 Å at the level of the proximal His92(F8). As a consequence, the heme is downshifted, and the Fe–CO bond is stretched being 1.9 Å in T-HbI, with respect to 1.7 Å in HbA. Again the distal His63(E7) weakly contacts the bound CO and adopts a conformation similar to the same topological residue in the α subunits.

previously determined by Fermi *et al.* and Baldwin.[27,28] The main-chain rmsd is 0.41 Å between the old and new deoxygenated structures and 0.49 Å between the two CO-bound structures; of course, the rmsd raises, respectively, to 1.25 Å and 1.45 Å taking into account all the side chains.

T-HbI in the deoxy and CO-bound states, solved at 2.3 and 2.5 Å resolution, respectively, correspond at the quaternary level to the T and R states. As pointed out by Tame *et al.*, a prominent difference relative to HbA is the much smaller pocket between the two β subunits.[11] In HbA, a positively charged cavity, lined by residues His2, Lys82 and His143, is the binding site for DPG and other phosphates.[19] In T-HbI, these residues are substituted by Glu2, Leu82 and Ser143[9,18]; moreover, the conformation of the first three residues of the β subunits (Val1, Glu2 and Trp3) hinders the rim of the pocket on both sides.[11]

The $\alpha_1\beta_1$ interface, made by residues belonging to the so-called BGH frame from the helices hosting the interacting residues, is quite extensive in both proteins and by-and-large insensitive to the ligation state (Table 1 and Supplementary Tables 1 and 4).

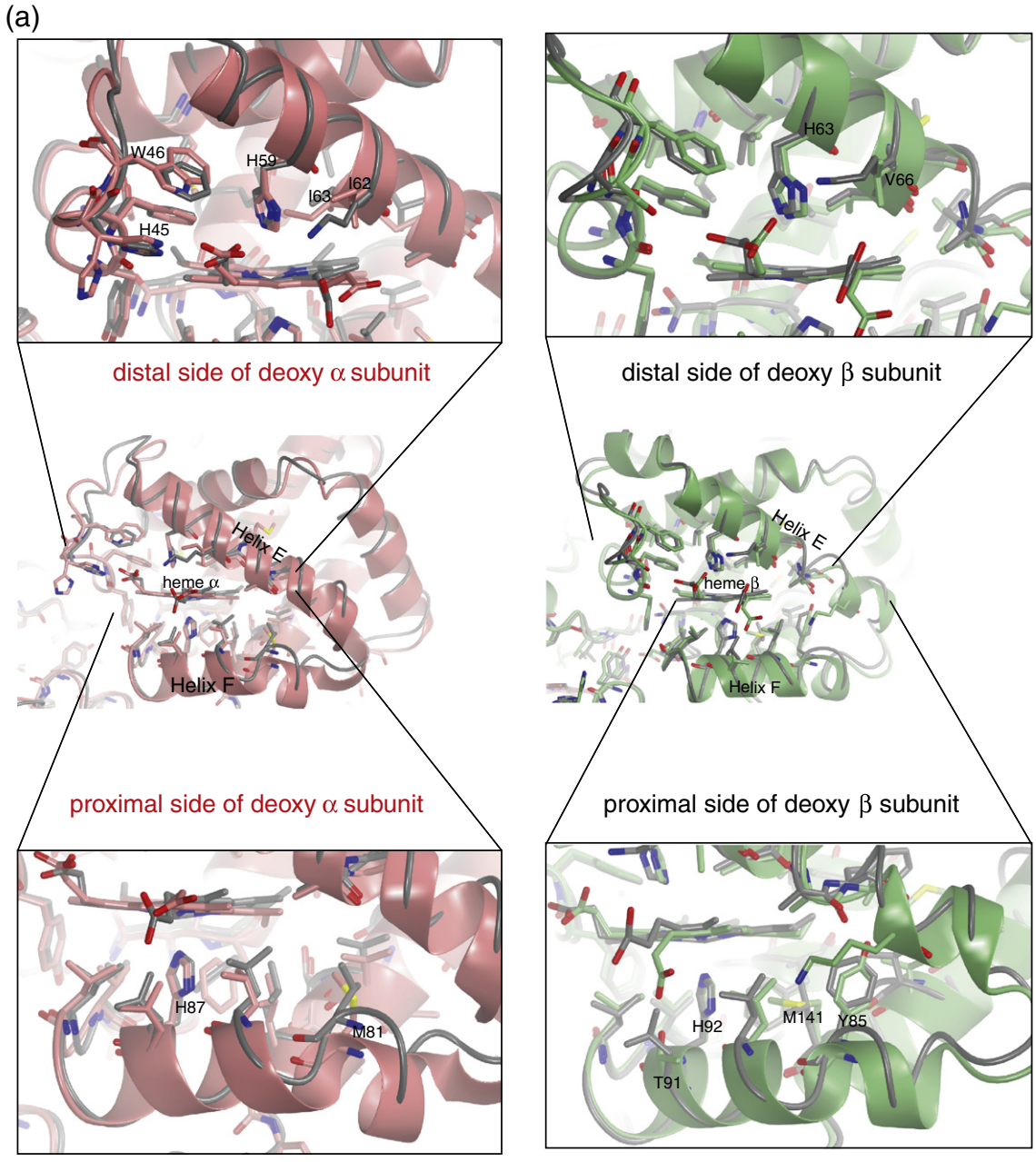

Fig. 1 (*legend on previous page*)

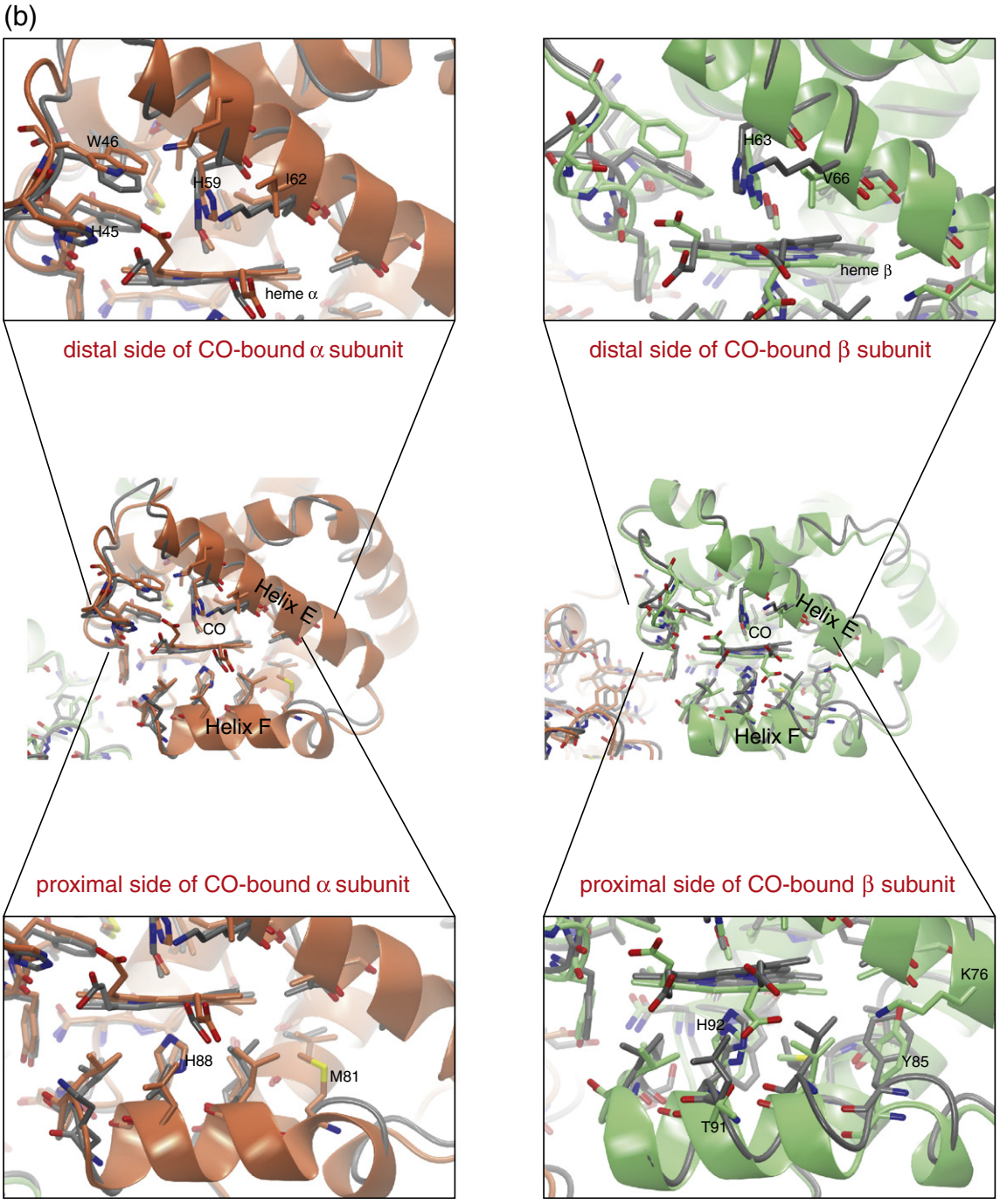

Fig. 1 (*legend on page 1516*)

Among the minor differences, in T-HbI, residue substitutions increase the hydrophobic complementary surface, hence attain a better packing of the interface.

The $\alpha_1\beta_2$ interface, contributed by contacts αC-βFG and αFG-βC of the C helix and the FG corner (plus a few residues coming from the C-terminus) of both participating subunits, is known to experience the largest quaternary shift. In tetrameric HbA, 584 Å^2 of buried surface are lost in going from deoxy to CO bound. On the contrary, in T-HbI, the quaternary transition increases the buried surface area of this interface by 613 Å^2 (Table 1). The key residues stabilizing this interface, that is βTrp37 and βArg40, are present in both proteins, but there are a few substitutions building a network of H-bond and salt bridges linking the $\alpha_1\beta_2$ and the $\alpha_1\beta_1$ interfaces (see

Supplementary Fig. 1 and Supplementary Tables 1–6 for a detailed description).

The heme pockets

In the deoxy α subunits, the heme pockets of HbA and T-HbI are clearly superimposable (main-chain rmsd 0.65 Å). Most residues are conserved but for a few substitutions in a critical zone of the distal pocket, which in T-HbI is coated with more hydrophobic residues (Fig. 1a). A notable feature consistent with an increased hydrophobicity is the absence of the water molecule normally seen in HbA.[12,27] The substitutions from HbA to T-HbI are as follows: Phe46→Trp46, Val62→Ile63, Lys61→Ile62 and Leu66→Ile67. In particular, Trp46 is prominent since it may assist the distal His59 in gating entrance to the pocket (Fig. 1a and Supplementary Fig. 2); moreover, Ile63 is bulkier than Val62. These structural peculiarities may suggest some hindrance to an incoming ligand with an effect on affinity. On the proximal side of deoxy T-HbI, there are only two substitutions (Leu80→Met81 and His89→Phe90). The topologically conserved Phe98 is in a different conformation, blocking a putative path from the distal to the proximal side of the heme. Noteworthy, the Fe-proximal His89 bond in T-HbI is 2.2 Å, essentially as in HbA.

The deoxy β subunits are also conserved and largely superimposable between HbA and T-HbI (main-chain rmsd 0.55 Å) (Fig. 1a). Once again, in the distal side, the residues in T-HbI are more hydrophobic or bulkier: Lys66→Val66, Leu68→Cys68, Phe71→Leu71, Tyr130→Trp130 and Leu134→Met134 (Fig. 1a); the latter three residues close a path presumed to allow diffusion of a gaseous ligand from the distal to the proximal side. The proximal side is also conserved but for residues Phe85→Tyr85, Cys93→Leu93, Leu141→Met141 and Leu91→Thr91. The first three substitutions almost completely fill up the proximal cavity in T-HbI and increase its hydrophobic character. Furthermore, the significant substitution of Leu91 with Thr91, in a topological position parallel with proximal His92, constrains the heme *via* a H-bond between the OH of Thr and one of the heme propionates (3.0 Å). This interaction, visible in Fig. 1a, is likely to help the proximal His92 to keep the heme domed in T-HbI. As in the α subunits, the Fe-proximal His92 bond is at 2.1 Å.

In the CO-bound state (Fig. 1b), the heme pocket of the α subunits of T-HbI displays some limited but significant structural changes with respect to HbA. The distal side is by-and-large superimposable, and Trp46 is still at H-bonding distance (3.5 Å) from the heme propionate, an interaction reinforced by His45 also in contact with the same propionate (3.3 Å). However, a significant finding is the distance between the distal His59 and the O of bound CO, which is 3.2 Å in T-HbI compared to 2.9 Å in HbA. The strain on the heme propionate from the distal side is only marginally transferred to the proximal side, the position of the F helix being almost unchanged and the Fe-proximal His89 bond being only slightly stretched (Fig. 1b).

The β subunits of the CO derivative of T-HbI are by-and-large similar to HbA, but once again, some interesting and possibly crucial features have emerged (Fig. 1b). On the proximal side, the F helix of T-HbI loses its ideal geometry and has a larger pass toward the center at the level of Tyr85, whose terminal OH atom superimposes on the top C atom of Phe85 present in HbA. This results in shrinkage of the whole F helix and loss of the H-bond (described above) between Thr91 and the heme propionate; the proximal His92 tends to follow the shift of the F helix. On the distal side, the most significant feature is that His63 is away from the oxygen atom of the CO (3.0 Å) and very mobile (*B* factor of 27 $Å^2$, with respect to a $\langle B \rangle$ of 20 $Å^2$ in the pocket), similarly to what seen for the α subunits (see above) and differently from HbA (B_{His} = 17 $Å^2$, as the average of the heme pocket). Another feature that may be of some relevance to account for the synergistic effect

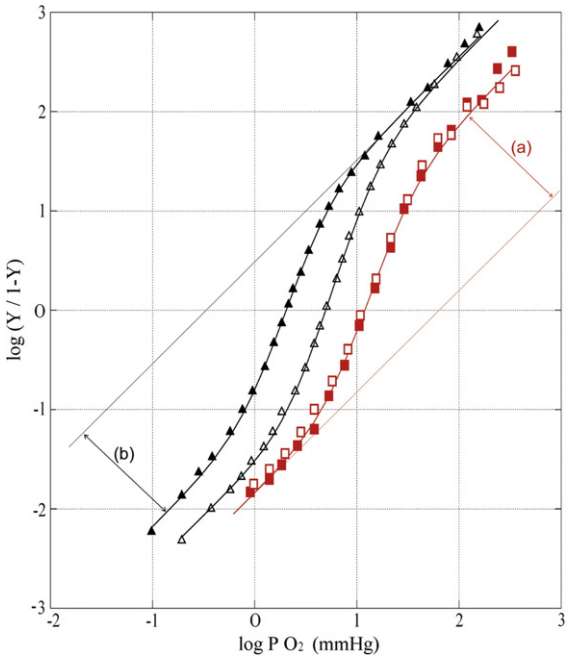

Fig. 2. Cooperative O_2 binding in HbA and T-HbI. The Hill plots of the O_2 equilibrium isotherms of HbA at pH 9.1+0.1 M Cl^- (filled triangles), HbA at pH 7.4+0.1 M Cl^- (open triangles) and T-HbI at pH 7.6 and 6.8 (red open and filled squares) are reported (see Table 3 for details). The distance between the high and low asymptotes is proportional to the free energy of interaction.[40] The figure shows that the free energy of interaction in T-HbI at pH 6.8–7.6 (a) is almost identical with that of HbA at pH 9.1 (b), but significantly smaller than that at pH 7.4 in the presence of Cl^- and DPG.

Table 2. Comparison between HbA and T-HbI

	HbA	T-HbI	Heterotropic ligand
α Chain	Val1 (NH1)	Ac-Ser1	Proton (Bohr effect)
α Chain	His122 (H5)	His123	Proton (Bohr effect)
β Chain	His2 (NH2)	Glu2	DPG
β Chain	Lys82 (EF6)	Leu82	DPG
β Chain	His143 (H21)	Ser143	DPG
β Chain	His146 (HC3)	Phe146	Proton (Bohr effect)

Amino acid substitutions directly linked to heterotropic allosteric effects. The topological positions are inserted in parenthesis.

of αTrp45 and βThr91 in T-HbI comes from the observation that these two residues lie on the same three-dimensional plane. In fact, we need to recall that the tetrameric assembly of hemoglobin arises from pairs of subunits being symmetrically arranged by 180° rotation, implying that the proximal side of one subunit is on the same plane as the distal side of the adjacent subunit. This assembly seems particularly effective along the $\alpha_1\beta_2$ interface in order for a "message" to spread from one heme pocket to another.

Moreover, it could be worth recalling that, in HbChico,[29] a natural mutant of HbA displaying low O_2 affinity, βLys66(E10) is replaced by Thr. In the α and β subunits of T-HbI, Lys in topological position E10 is substituted by Ile. A long basic residue in this position might restrain the distal His freedom to gate entrance/exit to the heme pocket, favoring ligand binding geometry, while a small hydrophobic residue would resort in the opposite effect. Finally, in both α and β subunits, there is a longer than usual Fe–CO bond (1.9 Å in T-HbI *versus* 1.7 Å in HbA), which suggests that the CO affinity of T-HbI in the R state should be lower than that of HbA, explaining the data published by Wyman *et al.*[30]

Oxygen binding analysis

The ligand binding properties of HbA and T-HbI are, at face value, similar yet very different as may be seen from a glance at Fig. 2. Cooperativity of the O_2 binding isotherm of HbA and its overall affinity are known to be dependent on pH and solvent composition (including DPG, IHP, ATP and PLP).[8,19,31] On the other hand, O_2 binding in T-HbI is cooperative yet the Hill plot and ligand affinity are totally independent of pH and solvent composition including organic phosphates.[9,10,13,14] This peculiarity, and particularly the absence of the Bohr effect, was taken as the paradigmatic case of molecular adaptation to physiological requirements; Brunori proposed that fast-swimming fishes need an O_2 carrier that is cooperative but pH independent to allow O_2 delivery even when blood pH drops significantly due to strenuous swimming for survival.[9] The absence of heterotropic effects in T-HbI proved to be the best independent evidence for the role of a limited number of well-identified amino acids in HbA, which were proposed by Perutz[2,19,32,33] to be involved in the Bohr effect and in the binding of DPG. As shown in Table 2, these residues in T-HbI are different or chemically modified.

A selection of relevant parameters obtained from fitting to the MWC model the ligand binding data of HbA and T-HbI is assembled in Table 3. Examination shows that the binding isotherms of HbA at pH 9.1 (in the presence of 0.1 M NaCl) and that of T-HbI (under all conditions) yield approximately the same MWC basic parameters. Thus, the equilibrium constant $L_0 = [T_0]/[R_0]$ is 2700 for HbA at pH 9.1 and 3000 for T-HbI, and the corresponding values of $c = K_R/K_T$ are 55 for the former and 40 for the latter. Moreover, for "stripped" HbA at pH 9.1, these parameters are remarkably close to those of T-HbI ($c = 41$; $L_0 = 3700$) (see Ref. 31). As widely known,[26,31] the allosteric properties of HbA are very different at physiological pH and with 2 mM DPG (e.g., $c = 380$ and $L_0 = 3 \times 10^6$), while no effect of this kind is seen for T-HbI.

Another most remarkable property of T-HbI, relative to HbA, is the lower O_2 affinity of the R state, the top asymptote of the Hill plot being clearly shifted to the right (Fig. 2). The molecular basis for this clear-cut drop in affinity of the subunits of R state T-HbI (~10-fold) is consistent with the structure of the distal side of the α and β subunits of the CO

Table 3. Functional parameters for O_2 binding to HbA and T-HbI

Protein (temperature)	Buffer conditions	K_T (M^{-1})	K_R (M^{-1})	K_R/K_T	p_{50} (mmHg)	Hill n_{max}	L_0 (T_0/R_0)	Reference
HbA (25 °C)	pH 7.4+0.1 M Cl^-	1.35×10^4	185×10^4	138	5.3	3.0	8.7×10^4	31
HbA (25 °C)	pH 7.4+0.1 M Cl^- +2 mM DPG	0.45×10^4	170×10^4	380	14.0	3.1	3.0×10^6	31
HbA (25 °C)	pH 9.1+0.1 M Cl^-	3.36×10^4	187×10^4	55	2.1	2.7	2.7×10^3	31
T-HbI (20 °C)	0.2 M bisTris (pH 6.8–7.6)	0.65×10^4	26×10^4	40	12.0	2.0–2.2	3.0×10^3	15

Data from Imai[31] and Brunori *et al.*,[15] obtained at protein concentrations around 1 mM heme (from 0.5 up to 2 mM). Under all conditions, dissociation of the tetramer into αβ dimers can be neglected, T-HbI being ~100-fold more stable than ligand-bound HbA.[17] Moreover, O_2 (and CO) binding to T-HbI is independent of pH from 6 to 9 (see also Fig. 2), and it is not affected by DPG, ATP, IHP and PLP[14]; the effect of Cl^- 0.3 M is to shift p_{50} from 12–13 mmHg (isoionic, pH 7.72) to 14–15 mmHg.[13]

derivative (see Fig. 1b), and particularly significant is the finding that, in both subunits, the distance between the distal His and the bound CO is increased compared to HbA (3.0–3.2 Å *versus* 2.8–2.9 Å, respectively). This structural peculiarity and the increased length of the Fe–CO bond (1.9 Å; see above) appear to account for the substantial increase in the rate constant for the dissociation of both O_2 and CO from R state T-HbI compared to HbA. In fact, for the latter protein, the canonical values are 15 s^{-1} for O_2 and 0.01 s^{-1} for CO,[8] while for the former, the corresponding rate constants are 175 s^{-1} and 0.28 s^{-1}, respectively.[15,17,30]

The salt bridges and other interactions

In his seminal 1970 paper, Perutz highlighted the significance of *eight salt bridges* present in deoxy HbA (T state) and broken in oxy HbA (R state), in controlling function[2] (see also Refs. 21 and 23). He assigned a specific role to six inter-subunit salt bridges per tetramer that are detectable only in the structure of the T state, that is, four connecting the two α subunits (α_1 and α_2) and two more connecting the α and β subunits across the $\alpha_1\beta_2$ and $\alpha_2\beta_1$ dimers. Moreover, he pointed out the presence of one additional O_2-linked intra-subunit salt bridge in each of the two β subunits (β_1 and β_2). Later on, Arnone and Arnone and Perutz discovered that several charged residues in the central cavity between β_1 and β_2 are crucial in the binding of DPG, which is indeed released upon the quaternary transition from T_0 to R_4.[33,34]

According to Perutz, the salt bridges have a role in accounting (at least partially) for the low affinity of the T state by imposing a tension at the heme.[2,19] Moreover, the relative stability of T_0 over R_0 depends on these salt bridges, some of which are also responsible for the Bohr and the DPG effects (see above). This mechanism was extended by Szabo and Karplus[20] and subsequently by Lee and Karplus[35] and Lee *et al.*,[36] who presented a thermodynamic formulation of Perutz's mechanism introducing an explicit "strength" for the salt bridges. These authors concluded that (i) the "strength" is not the same for all salt bridges and that (ii) the low affinity of the T state not only is constrained by the salt bridges but also must involve a strain in the so-called "allosteric core".

Perutz initially assigned a specific role for the Bohr effect to the interaction of the carboxylate of α_1Arg141 with the α-amino group of α_2Val1.[2] However, subsequent structures[12,27] indicated that these two residues lie 3.5–4 Å apart; hence, this interaction is possibly weaker than Perutz had estimated. A closer contact, presumably indicating stronger interaction, is seen in between the above-mentioned carboxylate of α_1Arg141 and α_2Lys127, to which we refer in this study.

The schematic comparison of the distribution of salt bridges in HbA and T-HbI, depicted in Fig. 3, provides the basis for our attempt to re-evaluate their role in cooperative O_2 binding and relative stability of the two allosteric states. Based on data discussed above (Table 3), it may be profitable to compare data for HbA at pH 9.1 (+0.1 M Cl^-) with T-HbI (at all pH values), recalling that also "stripped" HbA at pH 9.1 is similar to T-HbI ($c=41$; $L_0=3700$), quite apart for absolute O_2 affinity. An extensive legend to Fig. 3 details all the salt bridges and distances between the residues involved, indicated in the figure panels.

In the case of HbA, the two salt bridges (per tetramer) across the $\alpha_1\beta_2$ interface (α_1K40–β_2H146) break in going from T_0 to R_4; likewise, also the four salt bridges across the $\alpha_1\alpha_2$ interface (α_1R141 facing α_2D126 and α_2K127) break, summing up to a total of six. However, in HbA-CO, two novel salt bridges between β_1H146 and β_2V1/H2 (Fig. 3b′) are formed (2.8 Å). Thus, at pH 9.1, we count a net of four to six salt bridges per tetramer break in going from deoxy to liganded; if they were energetically equivalent (say at 1.5 kcal mol^{-1}), the sums may be compared to the difference in stability between the two allosteric states (L_0 from 2.700 to 3.700; Table 3).

In the case of T-HbI, the four salt bridges across the $\alpha_1\alpha_2$ subunits (α_1R142 facing α_2D127 and α_2K128 and their symmetrical) are poorly or not at all coupled to the allosteric transition; thus, they do not contribute to the thermodynamic balance sheet. On the other hand, the four across the $\alpha_1\beta_2$ interface (i.e., α_1D95–β_2W37 and α_1K40–β_2F146) break in going from T_0 to R_4; however, the latter is likely to be somewhat weak given that the distance is 3.5 Å (Fig. 3d). Examination of the structure of T-HbI-CO shows that two inter-subunit interactions (involving β_1F146 and β_2K135) are formed upon ligand binding, but once again, they are likely to be much weaker (see Fig. 3d′). In summary, attempting a thermodynamic balance sheet to account for an allosteric constant of $L_0=3.000$ (corresponding to a free-energy difference of ~5 kcal per tetramer), we may consider a contribution from two to less than four salt bridges per tetramer.

Concluding remarks

Allostery is an elegant solution to the thermodynamic and physiological problem of introducing cooperativity in biological macromolecules,[37] and there is no doubt that many, if not all, cooperative O_2 carriers resort to this structural mechanism.[21,31,32,38] A fundamental feature of the allosteric control of cooperativity in hemoglobin, which was incompletely foreseen in the original formulation of the two-state model, is the double action of allosteric effectors that, besides biasing the quaternary equilibrium in favor of the low-affinity T state (i.e., increasing L_0),

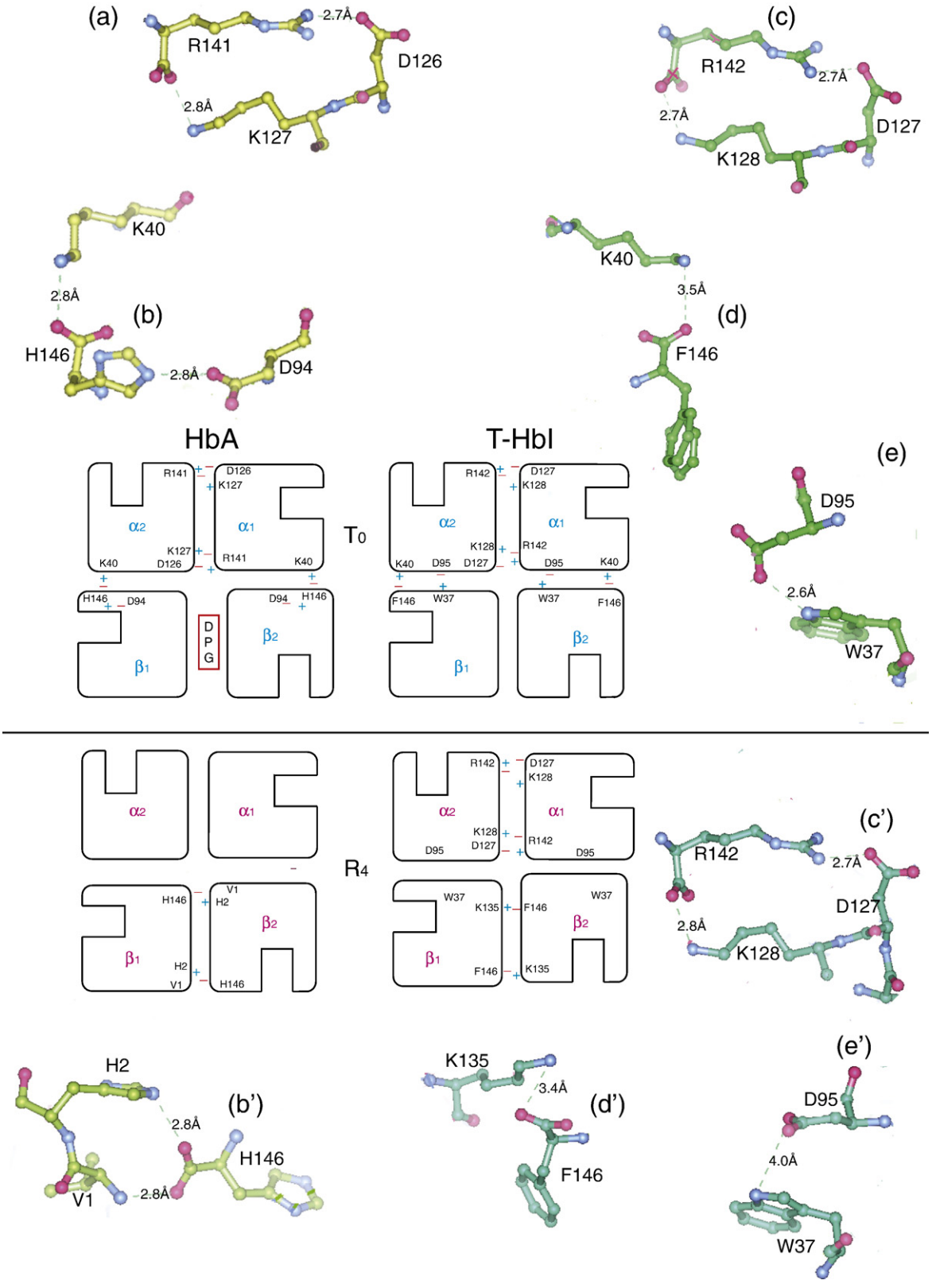

Fig. 3 (*legend on next page*)

also affect the O_2 affinity of the T state (by decreasing the value of K_T).[31,39] Only the former effect was predicted by Monod *et al.*[1] In order for cooperativity to be expressed under a wide array of experimental conditions and accounted for by allostery, three conditions must be met: (i) the two quaternary states should have different ligand affinity, (ii) the low-affinity state should be preferentially populated in the absence of ligands (i.e., $L_0 \gg 1$), and (iii) the high-affinity state should be preferentially populated in the presence of saturating ligand concentrations (i.e., $L_4 \ll 1$). If the only action of allosteric effectors were to increase the value of L_0, requirement (iii) would be met only over a limited range of experimental conditions, since L_4 is proportional to L_0 ($L_4 = L_0 \cdot K_T^4/K_R^4$). Indeed requirement (iii) implies that L_0 is matched by the ratio of the ligand binding constants of the two allosteric states.

Human Hb is a sophisticated molecular machine able to maintain cooperative ligand binding over a 100-fold range of absolute affinities and a 1000-fold (or greater) range of the allosteric constant L_0; its physiology relies on the fact that allosteric effectors control both L_0 and K_T.[19,20,31,39] As may be deduced from Fig. 2, the overall free energy of interaction at neutral pH and in the presence of DPG amounts to at least $\Delta G_0 = \sim 12$ kcal per tetramer, as calculated following Wyman[40] (see also Ref. 31). Therefore, the thermodynamic balance sheet indicates that, even counting the breakage of six salt bridges (at ~1.5 kcal each), the quaternary constraint on O_2 affinity requires further contributions, possibly involving differences in the organization of the $\alpha_1\beta_2$ interface over and above differential binding of DPG.

Trout HbI is quite different since it was selected to be insensitive to the environment (notably pH, DPG and temperature) and to respond only to the O_2 gradient, and indeed L_0, K_R and K_T yield cooperative ligand binding over a very restricted range of O_2 affinities.[9,10,15] However, T-HbI is in no way a "simple" machine, given that its O_2 affinity is sufficiently low to match physiological requirements,[9] achieving a result that, in most other hemoglobins, relies on allosteric effectors, at the price of being heavily dependent on the composition of the medium. What matters for the present discussion is the structural mechanism involved in this adaptation. In the analysis reported above, the specific functional properties of T-HbI have been traced to peculiar structural features, based on analysis of the crystallographic coordinates published by Tame *et al.*[11]

The complete absence of the Bohr effect and the DPG effect in T-HbI are well explained by a number of mutations and one chemical modification of the very residues identified by Perutz[2] as responsible for these heterotropic effects (see Table 2). The peculiar and physiologically relevant property emerging from a glance at the O_2 binding curves of T-HbI (Fig. 2) is the relatively low affinity of the R state[15] compared to HbA. This is mirrored by an ~20-fold increase in the rate of ligand dissociation from the R state observed for both O_2 and CO.[17,30] Analysis of the three-dimensional structures[11,12] unveils the molecular bases of this intrinsically lower ligand affinity of the R state of T-HbI that may be traced back to the mutations around the heme cavity of both α and β subunits; as discussed above (see Fig. 1b), the structure of the CO derivative of T-HbI highlights the increased distance

Fig. 3. A scheme of the salt bridges identified in HbA (left side) and T-HbI (right side), from analysis of the coordinates of deoxy HbA and HbA CO[12] and deoxy T-HbI and T-HbI CO.[11] The residues (single-letter code) are numbered, and signs (+/–) are placed close to them in order to highlight the polarity. In the scheme referring to the T_0 HbA tetramer, a box indicates the pocket for the binding of organic phosphates (red DPG box). All residues are then zoomed in the panels and represented in ball and stick, colored by atom coding, except for the carbons that are in gold for HbA and in green for T-HbI. **Top part of the scheme.** The following salt bridges are found in deoxy HbA (on the left). Between α_1 and α_2, a total of four salt bridges shown in (a): α_1R141–α_2K127 and its symmetric one, the C-terminus of α_1Arg141 interacts with N^ζ of α_2Lys127 (2.8 Å); α_1R141–α_2D126 and its symmetric one, the terminal NH_2 of α_1Arg141 contacts the COOH of α_2Asp126 (2.7 Å). In the interdimer ($\alpha_1\beta_2$) interface, shown in (b): α_1K40–β_2H146 and its symmetric one, α_1Lys40 N^ζ contacts the C-terminus of β_2His146 (2.8 Å); the intrachain β_2H146–β_2D94 and its symmetric one, the imidazole group of the C-terminal His146 makes an intrachain salt bridge with the COOH of Asp94 (2.8 Å). The following salt bridges are found in deoxy T-HbI (on the right). Between α_1 and α_2, a total of four shown in (c): α_1R142–α_2K128 and its symmetric one, also in this case the C-terminus of α_1Arg142 contacts the N^ζ of α_2Lys128 (2.7 Å); α_1R142–α_2D127 and its symmetric one, NH_2-terminus of α_1Arg142 binds the COOH of α_2Asp127 (2.7 Å). Across the interdimer ($\alpha_1\beta_2$) interface: α_1K40–β_2F146, shown as (d), where α_1Lys40 N^ζ faces the C-terminus of β_2Phe146 (3.5 Å) and its symmetric one, as well as α_1D95–β_2W37, α_1Asp95 COOH with N^ε of β_2Trp37 (2.6 Å) shown in (e) and its symmetric one. **Bottom part of the scheme.** The same schematic comparison as above is shown for the two CO-bound R_4 derivatives of HbA (bottom left) and T-HbI (bottom right). Upon ligand saturation, HbA looses six salt bridges. In particular, on the two α chains, the terminal residue Arg141 is more than 5 Å apart from both Lys127 (5.1 Å) and Asp126 (7.2 Å); α_2Lys40 is now freely exposed to the solvent. However, β_1His146 C-terminus is making one bond, with either β_2His2 or the N-terminus of β_2Val1 (2.8 Å) [see (b′)]. Therefore, only two are left (though reshuffled) in the R_4 state of HbA. In T-HbI, despite a quaternary conformational change, the termini of the α_1 and α_2 subunits remain unchanged [see (c′)] so that the same four salt bridges are maintained with the same distances and make no differential contribution. On the other hand, the four salt bridges across the $\alpha_1\beta_2$ and $\alpha_2\beta_1$ interfaces are now either broken (α_1K40–β_2F146) or severely weakened; the distance between COOH of α_1Asp95 and β_2Trp37 is now 4.0 Å [see (e′)]. β_1R146–β_2K135: the β_1-terminal residue Phe146 is now engaged in a weak salt bridge with N^ζ of β_2Lys135 (3.4 Å) [see (d′)].

between bound CO and the distal His (~3.0 to 3.2 *versus* ~2.7 Å for HbA) and the longer Fe–CO bond (at ~1.9 Å *versus* 1.7 Å for HbA), both consistent with the reduced R state affinity.

The relatively low value of $L_0 = 3.000$ is sufficient to warrant that the population of the T state in deoxy T-HbI exceeds that of the R state in the absence of O_2, but it is easily overcome in the presence of the gas. The difference in stability between the two allosteric states in the absence of ligands (~5 kcal mol^{-1}) may be compared with the ligand-linked breaking of an identified number of stereochemically sound salt bridges per tetramer. From analysis of Fig. 3, we conclude that definitely two (but possibly up to four) salt bridges may contribute, keeping in mind that they are likely to be energetically nonequivalent. Thus, we may say that the balance sheet (with a Δ of ~3 and 4.5 kcal per tetramer) is not inconsistent with the difference in stability between T_0 and R_0 but unlikely to be sufficient. Indeed the Hill plot of T-HbI (Fig. 2) yields an overall free energy of interaction of ~8 kcal per tetramer, which though smaller than that of HbA by ~30% clearly exceeds the contribution of the salt bridges outlined above, implying again that the quaternary constraint requires further contributions, possibly linked to different arrangements of the $\alpha_1\beta_2$ interface in the two allosteric states. In summary, we believe that we have a first-order consistency with previous analysis by Szabo and Karplus[20] and Lee and Karplus[35] on HbA, in so far as also in T-HbI the constraint on the O_2 affinity of the T state is only partially contributed by the salt bridges and must call for a strain extending to the so-called "allosteric core".

Materials and Methods

The coordinates of HbA in the deoxygenated and CO forms [Protein Data Bank (PDB) IDs 2dn2 and 2dn3] and those of T-HbI in the deoxygenated and CO-bound forms (PDB IDs 1out and 1ouu) were downloaded from the Protein Data Bank in Europe Repository at European Bioinformatics Institute†.[41]

The structures were inspected with Coot[42] and superimposed with SSM (*s*econdary-*s*tructure *m*atching),[43] and the calculations of the interface contact regions were carried out with the programs Areaimol[44,45] within the CCP4i suite.[46] The service protein interfaces, surfaces and assemblies PISA at European Bioinformatics Institute‡ was also used to inspect the interfaces and compute the free energy of stabilization.[47]

All the structural figures were made with CCP4mg.[48]

Acknowledgements

We would like to acknowledge all the researchers who have worked and are working on hemoglobin, dissecting its behavior from the physiological to the atomic view point, with the aim of understanding the "rules" of Nature. This work has been partially supported by grants from Fondo per gli Investimenti della Ricerca di Base (FIRB) Proteomica "RBRN07BMCT_007", International FIRB "RBIN06E9Z8" and Sapienza University of Rome under "Progetto Università" 2011 and 2012.

Conflict of Interest Statement. The authors declare to have no financial competing interests with the presented studies.

Supplementary Data

Supplementary data to this article can be found online at http://dx.doi.org/10.1016/j.jmb.2012.12.018

Received 31 October 2012;
Received in revised form 18 December 2012;
Accepted 20 December 2012
Available online 28 December 2012

Keywords:
human hemoglobin;
trout hemoglobin I;
crystal structure;
cooperativity;
salt bridges

†http://www.ebi.ac.uk/pdbe/
‡http://www.ebi.ac.uk/pdbe/prot_int/pistart.html

Abbreviations used:
MWC, Monod–Wyman–Changeux; DPG, 2,3-diphosphoglycerate; IHP, inositol hexaphosphate; PLP, pyridoxal 5′-phosphate; bisTris, 2-[Bis(2-hydroxyethyl) amino]-2-(hydroxymethyl)-1,3-propanediol; PDB, Protein Data Bank.

References

1. Monod, J., Wyman, J. & Changeux, J. P. (1965). On the nature of allosteric transitions: a plausible model. *J. Mol. Biol.* **12**, 88–118.
2. Perutz, M. F. (1970). Stereochemistry of cooperative effects in haemoglobin. *Nature*, **228**, 726–739.
3. Baldwin, J. & Chothia, C. (1979). Haemoglobin: the structural changes related to ligand binding and its allosteric mechanism. *J. Mol. Biol.* **129**, 175–220.
4. Frauenfelder, H., Sligar, S. G. & Wolynes, P. G. (1991). The energy landscapes and motions of proteins. *Science*, **254**, 1598–15603.
5. Daily, M. D. & Gray, J. J. (2009). Allosteric communication occurs via networks of tertiary and quaternary motions in proteins. *PLoS Comput. Biol.* **5**, e1000293.
6. Muirhead, H., Cox, J. M., Mazzarella, L. & Perutz, M. F. (1967). Structure and function of haemoglobin. 3. A three-dimensional Fourier synthesis of human deoxyhaemoglobin at 5.5 Ångstrom resolution. *J. Mol. Biol.* **28**, 117–156.

7. Perutz, M. F., Muirhead, H., Cox, J. M. & Goaman, L. C. (1968). Three-dimensional Fourier synthesis of horse oxyhaemoglobin at 2.8 Å resolution: the atomic model. *Nature*, **219**, 131–139.
8. Antonini, E. & Brunori, M. (1971). Hemoglobin and Myoglobin in Their Reactions with Ligands North Holland Publishing Co., London, UK.
9. Brunori, M. (1975). Molecular adaptation to physiological requirements: the hemoglobin system of trout. *Curr. Top. Cell. Regul.* **9**, 1–39.
10. Bellelli, A. & Brunori, M. (2011). Hemoglobin allostery: variations on the theme. *Biochim. Biophys. Acta*, **1807**, 1262–1272.
11. Tame, J. R. H., Wilson, J. C. & Weber, R. (1996). The crystal structures of trout Hb I in the deoxy and carbonmonoxy forms. *J. Mol. Biol.* **259**, 749–760.
12. Park, S. Y., Yokoyama, T., Shibayama, N., Shiro, Y. & Tame, J. R. (2006). 1.25 Å resolution crystal structures of human haemoglobin in the oxy, deoxy and carbonmonoxy forms. *J. Mol. Biol.* **360**, 690–701.
13. Airoldi, L., Brunori, M. & Giardina, B. (1981). Properties of trout HbI in water and ligand linked binding of Na^+. *FEBS Lett.* **129**, 273–276.
14. Brunori, M., Falcioni, G., Fortuna, G. & Giardina, B. (1975). Effect of anions on the oxygen binding properties of the hemoglobin components from trout (*Salmo irideus*). *Arch. Biochem. Biophys.* **168**, 512–519.
15. Brunori, M., Giardina, B., Colosimo, A., Coletta, M., Falcioni, G. & Gill, S. J. (1982). Thermodynamics and kinetics of the reactions of trout Hb I with O_2 and CO. In *Hemoglobin and Oxygen Binding* (Ho, C., ed.), Elsevier North Holland Inc., New York, NY.
16. Brunori, M., Giardina, B., Chiancone, E., Spagnuolo, C., Binotti, I. & Antonini, E. (1973). Studies on the properties of fish hemoglobin. Molecular properties and interactions with third components of the isolated hemoglobins from trout (*Salmo irideus*). *Eur. J. Biochem.* **39**, 563–570.
17. Giardina, B., Brunori, M., Binotti, I., Giovenco, S. & Antonini, E. (1973). Studies on the properties of fish hemoglobin. Kinetics of reaction with oxygen and carbon monoxide of the isolated hemoglobin components from trout (*Salmo irideus*). *Eur. J. Biochem.* **39**, 571–579.
18. Barra, D., Bossa, F. & Brunori, M. (1981). Structure of binding sites for heterotropic effectors in fish haemoglobins. *Nature*, **293**, 587–588.
19. Perutz, M. F. (1989). Mechanisms of cooperativity and allosteric regulation in proteins. *Q. Rev. Biophys.* **22**, 139–237.
20. Szabo, A. & Karplus, M. (1972). A mathematical model for structure–function relations in hemoglobin. *J. Mol. Biol.* **72**, 163–197.
21. Cui, Q. & Karplus, M. (2008). Allostery and cooperativity revisited. *Protein Sci.* **17**, 1295–1307.
22. Eaton, W. A., Henry, E. R., Hofrichter, J. & Mozzarelli, A. (1999). Is cooperative binding by hemoglobin really understood. *Nat. Struct. Biol.* **6**, 351–358.
23. Eaton, W. A., Henry, E. R., Hofrichter, J., Bettati, S., Viappiani, C. & Mozzarelli, A. (2007). Evolution of allosteric models for hemoglobin. *IUBMB Life*, **59**, 586–599.
24. Lukin, J. A. & Ho, C. (2004). The structure–function relationship of hemoglobin in solution at atomic resolution. *Chem. Rev.* **104**, 1219–1230.
25. Yonetani, T. & Laberge, M. (2008). Protein dynamics explain the allosteric behaviors of hemoglobin. *Biochim. Biophys. Acta*, **1784**, 1146–1158.
26. Bellelli, A. (2010). Hemoglobin and cooperativity: experiments and theories. *Curr. Protein Pept. Sci.* **11**, 2–36.
27. Fermi, G., Perutz, M. F., Shaanan, B. & Fourme, R. (1984). The crystal structure of human deoxyhaemoglobin at 1.74 Å resolution. *J. Mol. Biol.* **175**, 159–174.
28. Baldwin, J. M. (1980). The structure of human carbonmonoxy haemoglobin at 2.7 Å resolution. *J. Mol. Biol.* **136**, 103–128.
29. Bonaventura, C., Cashon, R., Bonaventura, J., Perutz, M., Fermi, G. & Shih, D. T. (1991). Involvement of the distal histidine in the low affinity exhibited by Hb Chico ($Lys^{\beta 66} \rightarrow Thr$) and its isolated β chains. *J. Biol. Chem.* **266**, 23033–23040.
30. Wyman, J., Gill, S. J., Noll, L., Giardina, B., Colosimo, A. & Brunori, M. (1977). The balance sheet of a hemoglobin. Thermodynamics of CO binding by hemoglobin trout I. *J. Mol. Biol.* **109**, 195–205.
31. Imai, K. (1982). Allosteric Effects in Haemoglobin Cambridge University Press, Cambridge, NY.
32. Perutz, M. F. & Brunori, M. (1982). Stereochemistry of cooperative effects in fish and amphibian haemoglobins. *Nature*, **299**, 421–426.
33. Arnone, A. (1972). X-ray diffraction study of binding of 2,3-diphosphoglycerate to human deoxyhaemoglobin. *Nature*, **237**, 146–149.
34. Arnone, A. & Perutz, M. F. (1974). Structure of inositol hexaphosphate–human deoxyhaemoglobin complex. *Nature*, **249**, 34–36.
35. Lee, A. W. & Karplus, M. (1983). Structure-specific model of hemoglobin cooperativity. *Proc. Natl Acad. Sci. USA*, **80**, 7055–7059.
36. Lee, A. W., Karplus, M., Poyart, C. & Bursaux, E. (1988). Analysis of proton release in oxygen binding by hemoglobin: implications for the cooperative mechanism. *Biochemistry*, **27**, 1285–12301.
37. Changeux, J. P. & Edelstein, S. (2011). Conformational selection or induced fit? 50 years of debate resolved. *F1000 Biol. Rep.* **3**, 19.
38. Perutz, M. F. & Imai, K. (1980). Regulation of oxygen affinity of mammalian haemoglobins. *J. Mol. Biol.* **136**, 183–191.
39. Yonetani, T., Park, S. I., Tsuneshige, A., Imai, K. & Kanaori, K. (2002). Global allostery model of hemoglobin. Modulation of O_2 affinity, cooperativity, and Bohr effect by heterotropic allosteric effectors. *J. Biol. Chem.* **277**, 34508–34520.
40. Wyman, J. (1964). Linked functions and reciprocal effects in hemoglobin: a second look. *Adv. Protein Chem.* **19**, 223–286.
41. Velankar, S., Best, C., Beuth, B., Boutselakis, C. H., Cobley, N., Sousa Da Silva, A. W. *et al.* (2010). PDBe: Protein Data Bank in Europe. *Nucleic Acids Res.* **38**, D308–D317.
42. Emsley, P., Lohkamp, B., Scott, W. G. & Cowtan, K. (2010). Features and development of Coot.

Acta Crystallogr., Sect. D: Biol. Crystallogr. **66**, 486–501.
43. Krissinel, E. & Henrick, K. (2004). Secondary-structure matching (SSM), a new tool for fast protein structure alignment in three dimensions. *Acta Crystallogr., Sect. D: Biol. Crystallogr.* **60**, 2256–2268.
44. Lee, B. & Richards, F. M. (1971). The interpretation of protein structures: estimation of static accessibility. *J. Mol. Biol.* **55**, 379–400.
45. Connolly, M. L. (1992). Shape distributions of protein topography. *Biopolymers*, **32**, 1215–1236.
46. Winn, M. D., Ballard, C. C., Cowtan, K. D., Dodson, E. J., Emsley, P., Evans, P. R. *et al.* (2011). Overview of the CCP4 suite and current developments. *Acta Crystallogr., Sect. D: Biol. Crystallogr.* **67**, 235–242.
47. Krissinel, E. & Henrick, K. (2007). Inference of macromolecular assemblies from crystalline state. *J. Mol. Biol.* **372**, 774–797.
48. McNicholas, S., Potterton, E., Wilson, K. S. & Noble, M. E. (2011). Presenting your structures: the CCP4mg molecular-graphics software. *Acta Crystallogr., Sect. D: Biol. Crystallogr.* **67**, 386–394.